

Effects of reduced discrete coupling on filament tension in excitable media

Sergio Alonso,^{1,a)} Markus Bär,¹ and Alexander V. Panfilov²

¹Physikalisch-Technische Bundesanstalt, Abbestrasse 2-12, 10587 Berlin, Germany

²Department of Physics and Astronomy, Ghent University, Krijgslaan 281-S9, B-9000 Gent, Belgium

(Received 16 July 2010; accepted 11 January 2011; published online 29 March 2011)

Wave propagation in the heart has a discrete nature, because it is mediated by discrete intercellular connections via gap junctions. Although effects of discreteness on wave propagation have been studied for planar traveling waves and vortexes (spiral waves) in two dimensions, its possible effects on vortexes (scroll waves) in three dimensions are not yet explored. In this article, we study the effect of discrete cell coupling on the filament dynamics in a generic model of an excitable medium. We find that reduced cell coupling decreases the line tension of scroll wave filaments and may induce negative filament tension instability in three-dimensional excitable lattices. © 2011 American Institute of Physics. [doi:10.1063/1.3551500]

Nonlinear waves account for many phenomena in spatially distributed chemical, physical, and biological systems. Often, vortex structures are formed, which can be spiral waves in two dimensions (2D) or scroll waves in three dimensions (3D). Spiral and scroll waves were first observed in chemical systems. Later, they were recorded in many other systems, including cardiac tissue, where they account for life threatening cardiac arrhythmias. In most of the systems nonlinear waves can be described using reaction–diffusion models. The study of spiral and scroll wave dynamics using numerical and analytical methods is a relevant topic in theoretical biology and nonlinear dynamics. One important direction of theoretical research is to identify mechanisms which can produce turbulence organized by multiple spiral or scroll waves. This is very important for cardiac tissue, where turbulence is associated with sudden cardiac death. Although there are several factors which facilitate the induction of turbulence, it occurs more easily in so-called remodeled cardiac tissue which is characterized by changes in ion channel expression and reduced electrical connections between cardiac cells. Some possible mechanisms which account for such observations have been identified. So far most of the related research is focused on possible 2D mechanisms. Here, we show numerically that a reduction in conduction may result in the onset of turbulence via a genuine 3D instability. We consider two cases: first an homogeneous reduction in conduction and second a random distribution of elements with reduced connectivity. We employ a generic model of excitable media in our study, which indicates a generic nature of this phenomenon. Thus, these findings potentially can be applied to any sufficiently discrete excitable system.

known as the filament, which governs the dynamics of these waves.¹ Usually, filaments exhibit positive filament tension: circular filaments, called scroll rings, shrink and disappear and straight filaments attain a stationary position in 3D slabs of excitable medium. Filaments, however, may have negative filament tension^{2–4} and under such conditions a chaotic dynamics is normally developed.^{5–7} Thus, filament tension is one of the most important determinants of 3D vortex dynamics in excitable media.⁸ The initial states of the filament tension instability have been observed in chemical systems.^{9,10}

Scroll waves are important for wave propagation and arrhythmias which occur in thick slabs of cardiac tissue, e.g., in ventricles of the heart. A propagating electrical wave of excitation initiates the contraction of the heart. Abnormal excitation of the heart may result in dangerous cardiac arrhythmias, including ventricular fibrillation, which is the main cause of sudden cardiac death. Excitation of the heart results from timed excitations of millions of individual heart cells coupled through highly conductive gap junctions.¹¹ As a result, on a small scale wave propagation is not continuous. It consists of fast propagation along individual cells and delays at intercellular connections during which excitation propagates between cells. In general, up to a half of the conduction time is a result of such gap junctional delays.¹²

Many forms of cardiac disease (e.g., ischemia, infarction, etc.) result in reduced numbers and conductivities of gap junctions, making the discrete nature of wave propagation more pronounced.^{11,12} Discrete effects of gap junctions were mainly studied for one-dimensional wave propagation.¹³ Reduced gap junction conductivities lead to a decrease of the wave velocity. As expected the increase of the inhomogeneity of the system typically produces the break up of the waves.¹⁴ However, studies of the effects of intercellular coupling on 2D vortexes, paradoxically showed that lower gap junctional conductance may prevent the formation of spatio-temporal chaos, due to the increase in the vortex period.^{15,16} There are different examples of stabilization by uncoupling of re-entries by heterogeneities with characteristic spatial scale smaller,¹⁶ similar,¹⁷ and larger¹⁸ than the spiral wave core.

I. INTRODUCTION

Scroll waves often form in three-dimensional excitable media. They rotate around a line of phase singularities,

^{a)}Electronic mail: Sergio.Alonso@ptb.de.

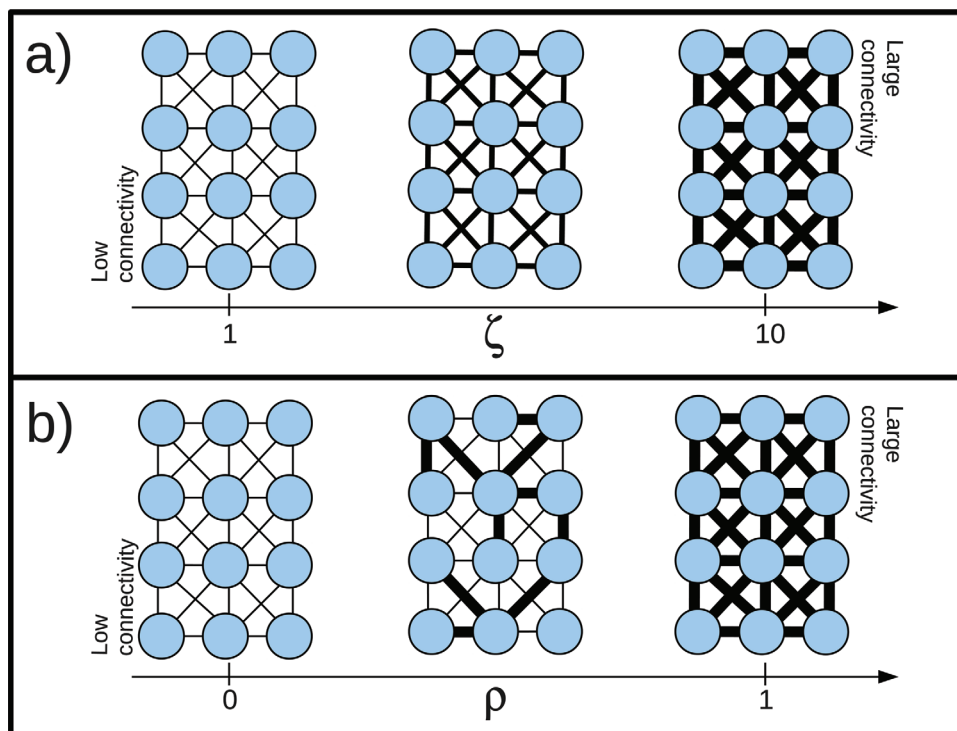


FIG. 1. (Color online) Sketch of the discretization of Eqs. (1) and (3) for the different approaches here considered. Circles represent the nodes of the grid and lines represent the connectivity between nodes. The thickness of the lines is proportional to the value of the conductivity (ζ). Two cases are considered: the change of the value of the conductivity ζ (a) and the fraction ρ of normal connectivities (b).

Furthermore, synchronization in 2D populations of chemical elements has been studied. Randomly distributed active chemical beads^{19,20} and periodic arrays of active droplets²¹ are examples of heterogeneous active chemical systems where pattern formation properties are determined by the discreteness of these elements. In such systems heterogeneous reaction–diffusion models have been employed for the study of wave propagation on heterogeneous chemical reactions.^{22,23}

Effects of discreteness on 3D vortices combined with fiber anisotropy have been previously discussed.^{8,24} Here, we study the effects of discrete wave propagation on the

tension of 3D scroll wave filaments in isotropic media. These effects could be enhanced by anisotropy.²⁵ We use two models of discrete tissue: (1) obtained from a uniform decrease of homogeneous intercellular conductance, see Fig. 1(a) and (2) obtained by a large effective reduction of the conductance on a fraction of randomly chosen cell connections, see Fig. 1(b). In both cases a decreased coupling results in a decrease of filament tension. Such a reduction may finally result in a qualitative change in the scroll wave dynamics: initially stable scroll waves may become unstable and result in spatio-temporal chaotic wave patterns. We explain the

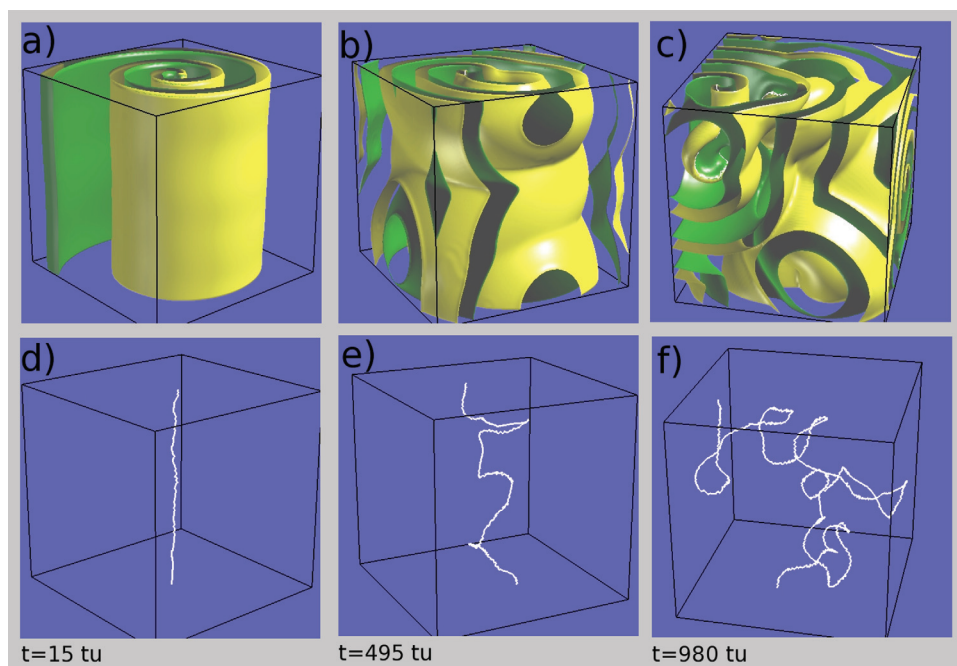


FIG. 2. (Color online) Negative filament tension instability due to reduced intercellular coupling. Evolution of the excitation waves (a–c) and filament (d–f) of a initially straight scroll wave for $\zeta = 1.875$. For the whole article we keep constant $a = 1.1$, $\epsilon = 0.02$ and $b = 0.15$ and $\Delta t = 0.015$. Size of the system: $100 \times 100 \times 100$.

observed effects by studying the period and wavelength of 2D spiral waves as a function of the discreteness. In both models a decreased coupling results in an increase of the period and wavelength of 2D spiral waves and, therefore, reduces the excitability of the tissue. Finally we discuss the implications of the results to cardiac applications.

II. MODELS

We consider a cubic grid of cardiac cells described by a generic (Barkley) model,²⁶ which has been widely used to study filament dynamics in 3D excitable media.²⁷ We decrease the connectivities among the cells in two different ways (see Fig. 1) giving rise to two discrete models referred to as the homogeneous discrete model and the dichotomic model, respectively. The equations of the homogeneous discrete model correspond to the discretization resulting from the 19-point approximation of the Laplacian^{5,6} at large connectivity. Such expression of the Laplacian considers first and second neighbors (see Fig. 1).

The equations are integrated with a second order Runge–Kutta method employing $\Delta t = 0.015$. Smaller temporal discretization does not affect the results. The system is discrete and all lengths are measured in terms of the distance between two consecutive elements.

A. Homogeneous discrete model

Cardiac cells connected by gap junctions are modeled by the following equations:¹⁶

$$\begin{aligned} \dot{V}_i &= R_V(V_i, I_i) + \zeta L(V_i, V_j), \\ \dot{I}_i &= R_I(V_i, I_i), \end{aligned} \quad (1)$$

where the variable V corresponds to the membrane action potential of a cell i and R_V represents total current across the cell membrane. Variable I represents the slow inward current responsible for tissue recovery. The reaction terms are given by the expressions $R_V = \epsilon^{-1} V(1 - V) (V - (I + b)/a)$ and $R_I = V - I$.²⁶ The parameter values on the reaction terms determine the excitability of the medium. The spatial operator $L(V_i, V_j)$ for large values of ζ is related with the discrete version of the Laplacian operator ($L(V_i, V_j) = \nabla \cdot (\nabla V) \Delta x^2$) with $\Delta x = 1$ (distance between two consecutive elements) and with 19-intercell connections defined on a cubic grid

$$L(V_i, V_j) = \sum_j^n \frac{2}{6} (V_j - V_i) + \sum_j^{nn} \frac{1}{6} (V_j - V_i), \quad (2)$$

where the index n (nn) corresponds to first (second) neighbors. For some simulations we use the analogous 2D representation. ζ is the parameter scaling intercellular conductivity. In the following we will refer to this approach as homogeneous discrete description.

B. Dichotomic model

Alternatively, we have considered a dichotomic heterogeneous coupling among cells in cardiac tissue, which allows a description of the effects of a decreased number of intercel-

lular connections. We study a model in which the decrease of intercellular coupling is achieved by a random weakening of a percentage of the intercellular connections

$$\begin{aligned} \dot{V}_i &= R_V(V_i, I_i) + \zeta L_{ij}(V_i, V_j), \\ \dot{I}_i &= R_I(V_i, I_i), \end{aligned} \quad (3)$$

where the connectivity matrix depends on the points:

$$L_{ij}(V_i, V_j) = \sum_j^n \eta_{ij} \frac{2}{6} (V_j - V_i) + \sum_j^{nn} \eta_{ij} \frac{1}{6} (V_j - V_i). \quad (4)$$

A fraction ρ of connections has a connectivity $\eta_{ij} = \eta_o = 1$ and the rest of connections $(1 - \rho)$ have a reduced connectivity $\eta_{ij} = \eta_r = 0.1$. The limits $\rho = 0$ and $\rho = 1$ correspond, respectively, to $\zeta = \zeta_r = 1$ and $\zeta = \zeta_o = 10$ in the previous model (see Fig. 1). This description has been previously employed in simple bistable media^{28,29} and similar prescription with $\eta_r = 0$ in wave propagation along cardiac tissue^{16,30} In the next section, we will refer to this approach as dichotomic model.

III. RESULTS

A. Wave dynamics in the homogeneous discrete model

A reduced intercellular coupling has a pronounced effect on the filament tension. It decreases the tension of the scroll wave filament and may result in the onset of scroll wave turbulence. An example of such unstable dynamics is shown in

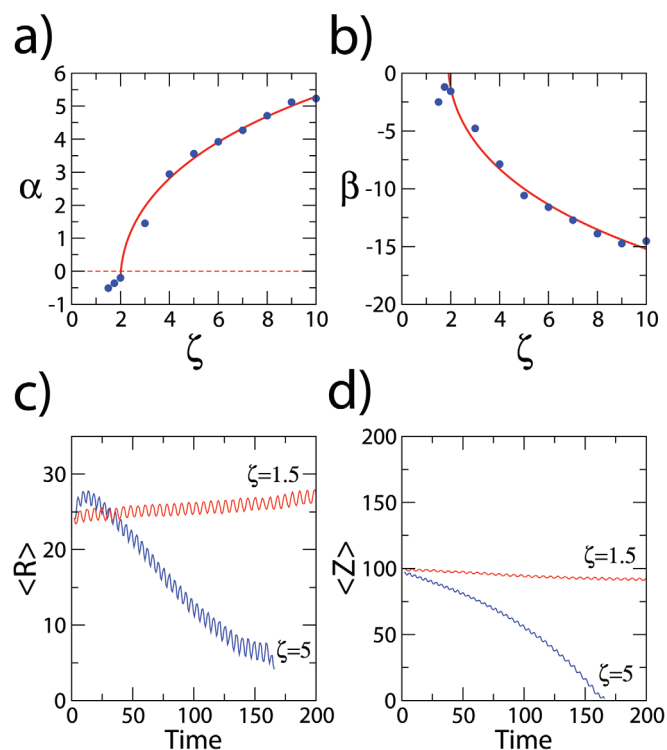


FIG. 3. (Color online) Dependence of the filament tension (a) and vertical drift (b) of scroll rings on ζ . Solid lines correspond to nonlinear fits. Evolution of the averaged three-dimensional radius (c) and vertical drift (d) for two values of ζ . Size of the system: $100 \times 100 \times 200$.

Fig. 2. The initial condition is a traveling wave with a free edge and with a slightly random perturbation which rapidly gives rise to an almost straight scroll wave. The parameters used correspond in the continuous limit to filaments with positive tension;^{5,6} therefore, a straight scroll wave similar to the one shown in Fig. 2(a) is stable. If the intercellular connections are homogeneously reduced, the filament attains negative tension and becomes unstable. As a result the perturbed filament shown in Fig. 2(d) grows in length, bends [Figs. 2(d) and 2(e)], and splits at the boundaries. Finally, an irregular regime [Fig. 2(c)] with a snaking filament is formed [Fig. 2(f)]. This process is similar to the patterns observed during the long wavelength instability of filaments with negative filament tension.^{6,31,32}

This instability occurs as a result of negative filament tension, as is illustrated in Fig. 3(a). This figure shows the effect of intercellular coupling on the main coefficients determining curvature dependent filament drift.³³ As was shown numerically² and analytically,³³ filament curvature induces drift of the filaments which has components in the normal (v_N), and in the binormal direction (v_B). Both velocities are directly proportional to the curvature (κ) of the filament:

$$v_N = -\alpha\kappa, \quad v_B = \beta\kappa. \tag{5}$$

These expressions are reduced for the particular case of scroll rings, waves rotating around a circular filament of radius R :

$$v_N = \frac{-\alpha}{R}, \quad v_B = \frac{\beta}{R}, \tag{6}$$

which permits the numerical calculation of the dependence of coefficients α and β on intercellular coupling, as it is shown in Fig. 3. Positive α produces the reduction of the filament length. It corresponds to positive filament tension (shrinking of circular filaments) and stabilizes straight filaments in slabs of cardiac tissue. Negative α corresponds to negative filament tension (expansion of circular filaments) and destabilizes straight filaments. In order to find the dependency of the coefficient α of the intercellular coupling, we initiated circular filaments (scroll rings) with the same initial radius for different values of ζ and follow their evolution. Two characteristic examples of such evolutions are shown in Figs. 3(c) and 3(d). For large coupling ($\zeta = 5$) after an initial transient the scroll ring shrinks while for low coupling ($\zeta = 1.5$) the scroll ring grows. From these dynamics

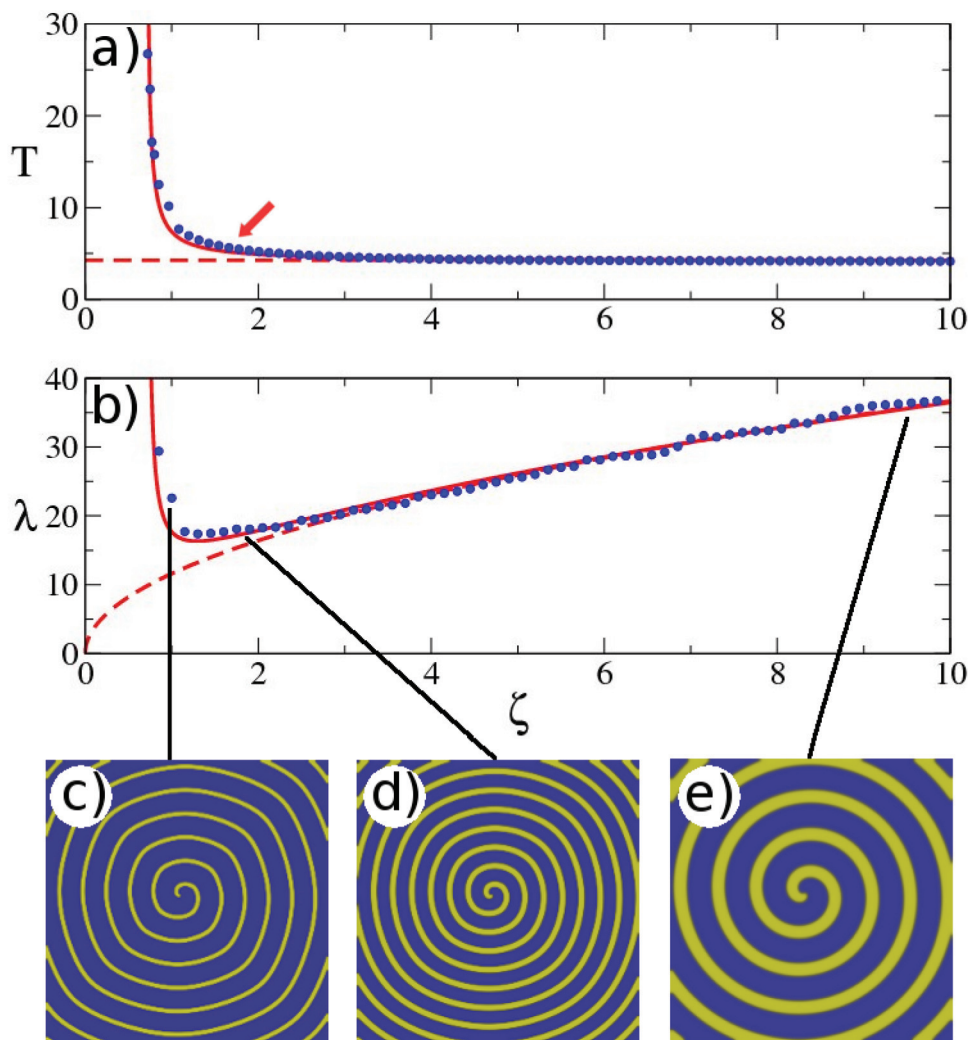


FIG. 4. (Color online) Dependence of the characteristic period (a) and wavelength (b) of spiral waves on the parameter ζ . Dashed lines show the expected continuous limits and solid lines are non-linear fits. Arrow indicates the value employed for 3D simulations in Fig. 2. Three snapshots corresponding to the spiral waves with $\zeta = 1$ (c), $\zeta = 1.8$ (d), and $\zeta = 9.3$ (e). Size of the system: 256×256 .

we computed the values of the coefficient α [Fig. 3(a)]. For large values of intercellular coupling ζ scroll rings contract (α is positive). If the intercellular coupling decreases the velocity of contraction decreases and for $\zeta < 2.2$ the filament starts expanding (α is negative). As a result, scroll rings grow and the negative filament tension instability gives rise to irregular wave dynamics in 3D (Fig. 2). Similar results for the vertical drift are presented in Fig. 3(b) and show a progressive decrease of the drift speed with decrease of the intercellular coupling.

The points plotted in Figs. 3(a) and 3(b) are obtained by three-dimensional simulations. In a continuous medium the angular symmetry of scroll rings in cylindrical coordinates permits a reduction of the scroll ring motion to the dynamics in the two-dimensional plane (r, z) .^{2,5,6,34,35} Our cubic discrete grid does not have any angular symmetry and consequently this reduction is not applicable.

In order to understand the mechanism responsible for the decrease of filament tension we studied how the decrease of ζ affects the properties of 2D spiral waves. In Fig. 4 we plot the dependence of the characteristic period (T) and wavelength (λ) of spiral waves on the parameter ζ . Examples of spiral waves are shown in Figs. 4(c)–4(e). The spiral wavelength λ is determined by calculating the two-dimensional power spectrum of the spiral waves.

For large values of the intercellular coupling ζ , the period of spiral waves remains constant and we can see the expected square root dependence of the wavelength on the parameter ζ (dashed lines in Fig. 4) corresponding to the prediction for the continuous limit. For small values of the intercellular coupling ($\zeta < 3$) discreteness becomes relevant and period and wavelength of the spiral waves increase. This is a clear deviation from the continuous limit and has to be attributed to the discrete cell coupling. Such increase in period and the wavelength is typical for a medium with

decreased excitability. If $\zeta < 0.8$, the medium loses its excitable properties and cannot conduct excitation waves anymore. Thus, the decrease of the conductivity ζ causes an effective decrease in the excitability of the medium.⁶ Because low excitability of the medium results in negative filament tension (see, e.g., Ref. 6), it explains the results observed in Figs. 2 and 3.

B. Wave dynamics in the dichotomic model

We have also studied the filament dynamics in the dichotomic model. A fraction ρ of connections has connectivity $\eta_{ij}=1$ and the rest have a reduced connectivity $\eta_{ij}=0.1$. We found that results obtained using this approach are qualitatively similar to those obtained using the homogenized approach considered previously.

Figure 5 shows that a scroll wave which is stable for normal coupling ($\rho = 1$) may become unstable if a fraction of the couplings between cells is decreased. The filament length of the scroll wave grows and due to this negative filament tension instability we observe irregular wave behavior (Fig. 5). This is similar to the results obtained in Fig. 2 for the homogeneous discrete approach.

In Fig. 6 we plot the dependence of the characteristic period (T) and wavelength (λ) of spiral waves on the parameter ρ . Examples of spiral waves are shown in Figs. 6(c)–6(e). The effective reduction of the cell coupling for small values of ρ increases the period of spiral waves and only affects the wavelength slightly. In contrast with Fig. 4, the period of the spiral waves do not diverge because the limit value $\rho = 0$ in Fig. 6 corresponds to the value $\zeta = 1$ in Fig. 4 which produces a finite spiral period.

Using earlier results²⁹ one can calculate an effective homogenized conductivity of the medium (ζ_e) for different values of ρ from the implicit relation:

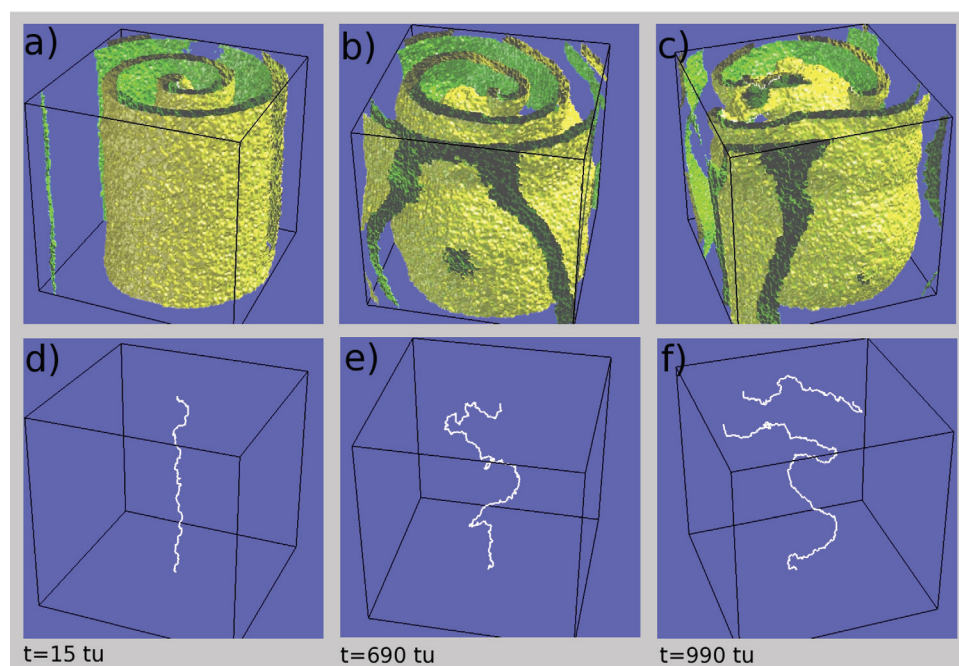


FIG. 5. (Color online) Negative filament tension instability due to heterogeneous intercellular coupling. Evolution of the excitation waves (a–c) and filament (d–f) of a initially straight scroll wave for $\rho = 0.25$. Size of the system: $100 \times 100 \times 100$.

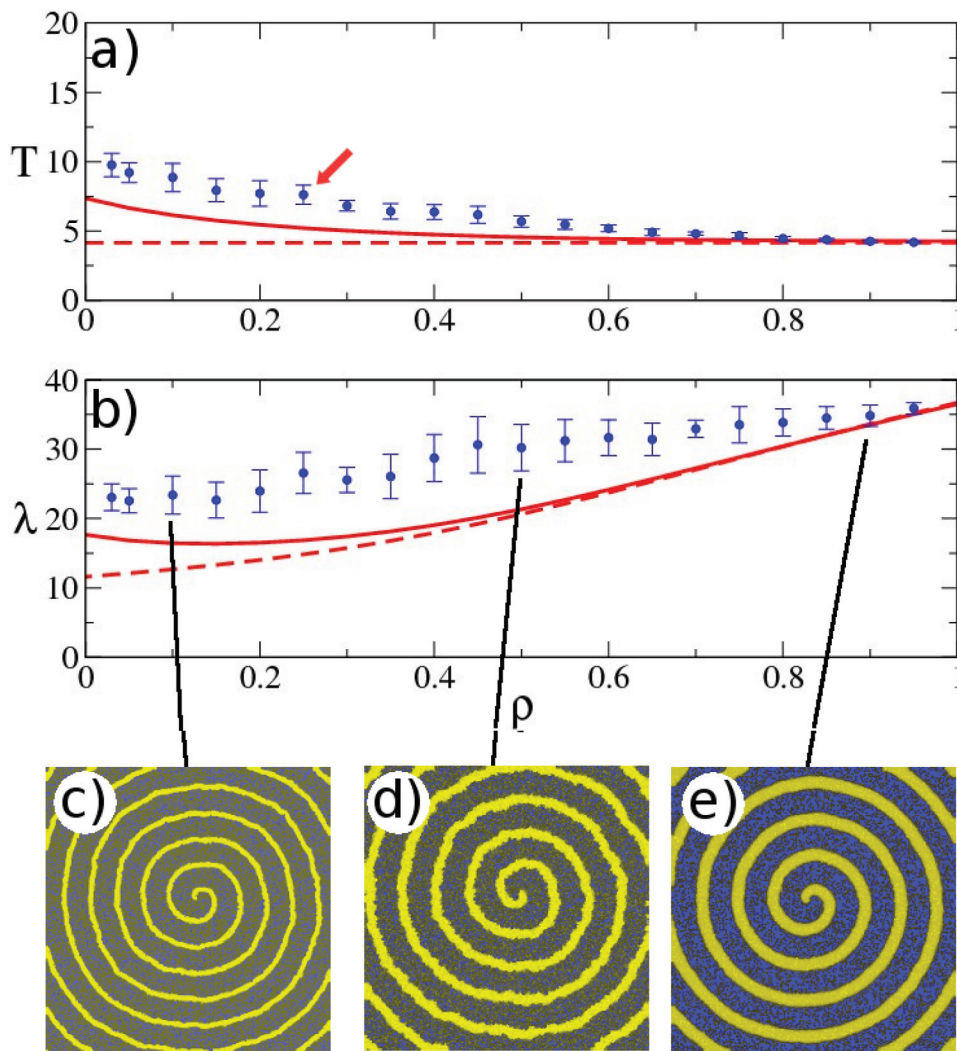


FIG. 6. (Color online) Dependence of the characteristic period (a) and length (b) of spiral waves on the fraction of normal connectivities ρ in a heterogeneous system. Points are average over ten realizations. Dashed and solid lines correspond, respectively, to the predictions with an effective conductivity ζ_e for continuous and discrete limits. Arrow indicates the value employed for 3D simulations in Fig. 5. Three snapshots corresponding to spiral waves with different values $\rho = 0.1$ (c), $\rho = 0.5$ (d), and $\rho = 0.9$ (e). Size of the system: 256×256 .

$$(1 - \rho) \frac{\zeta_o - \zeta_e}{\zeta_o + \zeta_e} + \rho \frac{\zeta_r - \zeta_e}{\zeta_r + \zeta_e} = 0, \quad (7)$$

and quantitatively compare the results of the homogenized and dichotomic approaches. Dashed lines in Fig. 6 show the prediction of periods and wavelengths of spiral waves for the continuous approach. Solid lines in Fig. 6 correspond to the discrete homogenized models. We calculate an effective conductivity $\zeta_e(\rho)$,²⁹ and we use this value to obtain T and λ in Fig. 4. We see a reasonable correspondence of theoretical and numerical results.

IV. DISCUSSION AND CONCLUSIONS

We show that a decrease of intercellular coupling results in the reduction of tension of scroll wave filaments and may result in negative tension leading to 3D turbulence. We achieve this decrease by a moderate homogeneous reduction of the coupling strength and by a large reduction of randomly chosen connections. The results of the two approaches are qualitatively similar: reduced coupling increases the period of the scroll waves and lowers the medium excitability leading to negative filament tension.

Here we use two simplified descriptions of discrete coupling. Exact reproduction of discrete effects is a difficult problem which requires detailed mapping of cell shapes and positions in 3D syncytium, obtaining information on the location of gap junctions of each individual cell and detailed modeling in intracellular and intercellular propagation. Currently there is an increase of attempts in this direction.^{36–38} Extension of this approach to realistic 3D cardiac geometry is not feasible as typical 3D simulation would require representations of more than 10^8 cells. However, there are already heterogeneous monodomain and bidomain models^{37,39} for small pieces of cardiac tissue. On the other hand, the results of Refs. 40 and 41 show that the homogenized and dichotomic approaches used here adequately reproduce known discrete effects of cardiac propagation of wave in cardiac cells coupled by discrete gap junctions. In this manuscript we show that both approaches essentially lead to decreasing filament tension. Therefore, we think that more detailed descriptions of tissue anatomy will not change the main qualitative result of our paper.

The decrease in filament tension is due to the decrease of excitability of the medium in response to reduced cell

coupling. Such a decrease in excitability should be present in any discrete model of excitable tissue and in experiments. Thus we expect that in other models or experiments, a progressive reduction of intercellular coupling will finally result in the onset of negative filament tension. This three-dimensional instability is observed in thick systems and cannot appear in thin slabs of tissue.³⁴ The instability appears at a critical size and it depends on the parameter values and how deep is the system into the negative filament tension region. The value of this critical size should be estimated in future research using physiologically realistic models for cardiac cells.

Although the models employed are generic, some of their joined properties reproduces important characteristics of waves in real cardiac tissue. In fact, discrete effects on wave propagation in such generic models become essential when the wavefront occupies one to two cells⁴² and the continuous description is accurate for wavefronts much larger than two cells. The size of the wave can be much larger than this limit, but the relevant quantity to evaluate the level of discreteness is the width of wavefront.²⁹ In real cardiac tissue the front width is of the order of 500 μm (i.e., four to five cardiac cells) for normal conduction, due to the fast activation time of the sodium current $\tau \approx 1$ ms and the fast speed of the waves $v \approx 0.5$ m/s.¹¹ In abnormal regimes, e.g., during re-entrant wave rotation, the velocity can be substantially slower and thus the wavefront may approach this one to two cells length estimate and the discrete effects studied in this article may become relevant. The validity of this dimensionless estimate for real experimental conditions needs to be further investigated in simulations involving more accurate description of the discrete effects and more detailed models of cardiac tissue.³⁴

It is likely that effects of discrete cell coupling on filament tension are more pronounced during pathological cardiac conditions, e.g., during ischemia when intercellular coupling is reduced. Also, many cardiac diseases result in a remodeling of cardiac tissue and fibrosis, which also effectively reduces intercellular coupling in cardiac tissue.^{11,13}

In summary, for the two versions of a generic model, with discrete and heterogeneous spatial coupling we have shown that a reduced connectivity between discrete elements decreases the tension of filaments of 3D scroll waves and may result in the onset of unstable turbulent dynamics.

ACKNOWLEDGMENTS

We are grateful to Boyce E. Griffith for a stimulating discussion. We acknowledge financial support from the German Science Foundation (DFG) within the framework of SFB 555 “Complex nonlinear processes,” and SFB 910 “Control of self-organizing nonlinear systems,” to the Insti-

tut des Hautes Études Scientifiques, Bures-sur-Yvette, France, and to the James Simons Foundation.

- ¹A. T. Winfree and S. H. Strogatz, *Physica D* **8**, 35 (1983).
- ²A. V. Panfilov and A. N. Rudenko, *Physica D* **28**, 215 (1987).
- ³P. K. Brazhnik, V. A. Davydov, V. S. Zykov, and A. S. Mikhailov, *Sov. Phys. JETP* **66**, 984 (1987).
- ⁴V. N. Biktashev, A. V. Holden, and H. Zhang, *Philos. Trans. R. Soc. London, Ser. A* **347**, 611 (1994).
- ⁵S. Alonso, F. Sagués, and A. S. Mikhailov, *Science* **299**, 1722 (2003).
- ⁶S. Alonso, F. Sagués, and A. S. Mikhailov, *Chaos* **16**, 023124 (2006).
- ⁷H. Henry and V. Hakim, *Phys. Rev. E* **65**, 046235 (2002).
- ⁸F. H. Fenton, E. M. Cherry, H. M. Hastings, and S. J. Evans, *Chaos* **12**, 852 (2002).
- ⁹C. Luengviriyai, U. Storb, G. Lindner, S. C. Müller, M. Bär, and M. J. B. Hauser, *Phys. Rev. Lett.* **100**, 148302 (2008).
- ¹⁰T. Bánsági and O. Steinbock, *Phys. Rev. E* **76**, 045202(R) (2007).
- ¹¹A. G. Kleber and Y. Rudy, *Physiol. Rev.* **84**, 431 (2004).
- ¹²V. G. Fast and A. G. Kleber, *Circ. Res.* **73**, 914 (1993).
- ¹³H. J. Jongsma and R. Wilders, *Circ. Res.* **86**, 1193 (2000).
- ¹⁴G. Bub, A. Shrier, and L. Glass, *Phys. Rev. Lett.* **94**, 028105 (2005).
- ¹⁵K. H. W. J. Ten Tusscher and A. V. Panfilov, *Europace* **9**, vi38 (2007).
- ¹⁶A. V. Panfilov, *Phys. Rev. Lett.* **88**, 118101 (2002).
- ¹⁷P. Bittihn, G. Luther, E. Bodenschatz, V. Krinsky, U. Parlitz, and S. Luther, *New J. Phys.* **10**, 103012 (2008).
- ¹⁸C. Cabo and P. A. Boyden, *Am. J. Physiol. Heart Circ. Physiol.* **291**, H2606 (2006).
- ¹⁹J. Masekko, J. S. Reckley, and K. Showalter, *J. Phys. Chem.* **93**, 2114 (1989).
- ²⁰A. F. Taylor, M. R. Tinsley, F. Wang, Z. Huang, and K. Showalter, *Science* **323**, 614 (2009).
- ²¹M. Toiya, H. O. Gonzalez-Ochoa, V. K. Vanag, S. Fraden, and I. R. Epstein, *J. Phys. Chem. Lett.* **1**, 1241 (2010).
- ²²R. Toth and A. F. Taylor, *J. Chem. Phys.* **125**, 224708 (2006).
- ²³X. Yuan, X. Lu, H. Wang, and Q. Ouyang, *Phys. Rev. E* **80**, 066201 (2009).
- ²⁴A. V. Panfilov and J. P. Keener, *Physica D* **84**, 545 (1995).
- ²⁵J. Mi and M. Ping, *Chin. Phys. Lett.* **26**, 074703 (2009).
- ²⁶D. Barkley, M. Kness, and L. S. Tuckerman, *Phys. Rev. A* **42**, 2489 (1990).
- ²⁷M. Dowle, R. M. Mantel, and D. Barkley, *Int. J. Bifurcation Chaos* **7**, 2529 (1997).
- ²⁸S. Alonso, R. Kapral, and M. Bär, *Phys. Rev. Lett.* **102**, 238302 (2009).
- ²⁹S. Alonso, M. Bär, and R. Kapral, *J. Chem. Phys.* **131**, 214102 (2009).
- ³⁰E. M. Cherry, J. R. Ehrlich, S. Nattel, and F. H. Fenton, *Heart Rhythm* **4**, 1553 (2007).
- ³¹V. N. Biktashev, *Int. J. Bifurcation Chaos* **8**, 677 (1998).
- ³²R. M. Zariwsky, S. F. Mironov, and A. M. Pertsov, *Phys. Rev. Lett.* **92**, 168302 (2004).
- ³³J. P. Keener and J. J. Tyson, *SIAM Rev.* **34**, 1 (1992).
- ³⁴S. Alonso and A. V. Panfilov, *Chaos* **17**, 015102 (2007).
- ³⁵S. Alonso and A. V. Panfilov, *Phys. Rev. Lett.* **100**, 218101 (2008).
- ³⁶M. S. Spach, J. F. Heidlage, P. C. Dolber, and R. C. Barr, *Circ. Res.* **86**, 302 (2000).
- ³⁷J. G. Stinstra, R. MacLeod, and C. S. Henriquez, *Ann. Biomed. Eng.* **38**, 1390 (2010).
- ³⁸S. F. Roberts, J. G. Stinstra, and C. S. Henriquez, *Biophys. J.* **95**, 3724 (2008).
- ³⁹C. Cabo and P. A. Boyden, *Biophys. J.* **96**, 3092 (2009).
- ⁴⁰R. M. Shaw and Y. Rudy, *Circ. Res.* **81**, 727 (1997).
- ⁴¹A. Pertsov, in *Discontinuous Conduction in the Heart*, edited by P. Spooner, R. W. Joyner, and J. Jalife (Futura Publishing Company, Armonk, 1997).
- ⁴²The width of the wavefront in units of “cell length” is estimated from the expression $\ell = 4\sqrt{2\zeta\epsilon}$, see Ref. 28.